Characterizing Composite of Multiwalled Carbon Nanotubes and POE-*g*-AA Prepared via Melting Method

Chin-San Wu

Department of Biochemical Engineering, Graduate Institute of Environmental Polymer Materials, Kao Yuan University, Kaohsiung County, Taiwan 82101, Republic of China

Received 14 September 2006; accepted 14 November 2006
DOI 10.1002/app.25839
Published online in Wiley InterScience (www.interscience.wiley.com).

ABSTRACT: Multiwalled carbon nanotubes (MWNTs) with acyl chloride functional groups and a metallocene polyethylene–octene elastomer (POE) or an acrylic acid-grafted metallocene polyethylene–octene elastomer (POE-*g*-AA) were used to prepare hybrids (POE/MWNTs or POE-*g*-AA/MWNTs) using a melting method, with a view to identify a hybrid with improved thermal properties. Hybrids were characterized using Fourier transform infrared spectroscopy, ^{13}C solid-state nuclear magnetic resonance, X-ray diffraction, thermogravimetry analysis, and scanning electron microscopy. MWNTs were purified using acid treatment, and results showed that —COOH of MWNTs increased with acid treatment time and leveled off after 24-h treatment. Much better dispersion and homogeneity of MWNTs was obtained with POE-*g*-AA in place of POE as the matrix. As a result, tensile strength at break of POE-*g*-AA/MWNTs was significantly improved even at 5 wt % MWNT content. Moreover, temperature of thermal decomposition for POE-*g*-AA/MWNTs was about 40–50°C higher than that for POE-*g*-AA, indicating higher thermal stability. This was because the carboxylic acid groups in POE-*g*-AA and the acyl chloride functional sites in MWNTs allow the formation of stronger chemical bonds. J Appl Polym Sci 104: 1328–1337, 2007

Key words: thermal properties; elastomers; nanocomposites

INTRODUCTION

Because of the promising physical, thermal, mechanical, and electric properties,[1,2] carbon nanotubes (CNTs) have attracted extensively scientific interest[3,4] recently. Moreover, applications of multiwalled carbon nanotubes (MWNTs) in structural materials such as polymer composites are more feasible with their mass production, which leads to price reduction.[5,6] Specifically, use of CNTs in polymer/carbon nanotube composites has attracted wide attention.[7,8] In this sense, it has been reported that the matrix properties can be effectively enhanced via the addition of CNTs in different polymer matrices.[9,10] Nevertheless, using CNTs as filler in polymer matrix, disadvantageous effects were observed due to aggregation and nonuniform dispersion of CNTs in common solvents. Therefore, two primary conditions are required for application of CNT nanocomposites: the homogeneous dispersion of CNTs in the host matrix and the interfacial interaction. Recently, various methods have been introduced for functionalizing CNTs to improve their compatibility with monomers and polymers.[11–14] Among these methods, most involve oxidation of the surfaces of single-walled carbon nanotubes (SWNTs) or multiple-walled carbon nanotubes (MWNTs).[15–18] For example, the functional groups are often generated by the chemical oxidation of MWNTs in a mixture of sulfuric and nitric acids or by the treatment of MWNTs with piranha (sulfuric acid/hydrogen peroxide). In a mixture of strong oxidizing acids such as HNO_3 or H_2SO_4,[19,20] CNTs can be functionalized with carboxyls or quinines. Additionally, dangling bonds on MWNTs are generated in organic solvents, conferring ability of further chemical reactions.[21,22] Dispersion of oxidized MWNTs in solvents or polymer matrices can be further enhanced by the grafting of organic polymers onto their surfaces. Hill et al.[23] declared the effectiveness of functionalized CNTs with a polystyrene copolymer by the esterification of carboxylic acid-functionalized nanotubes. Comprehensively, various methods proposed include either growing polymers from negatively charged carbon nanotubes or anchoring polymers onto chemically oxidized carbon nanotubes.

On the other hand, among the polymer matrices, polyolefins are the most widely used thermoplastics because of their well-balanced physical and mechanical properties and their easy processability at a relatively low cost that makes them a versatile material.[24,25] Thermoplastics can be toughened by rubbers and the blends, commonly called thermoplastic elastomer polyolefins (TPOs), are a class of materials that combine the good processing characteristics of thermoplastics at elevated temperatures and play an

Correspondence to: C.-S. Wu (cws1222@cc.kyu.edu.tw).

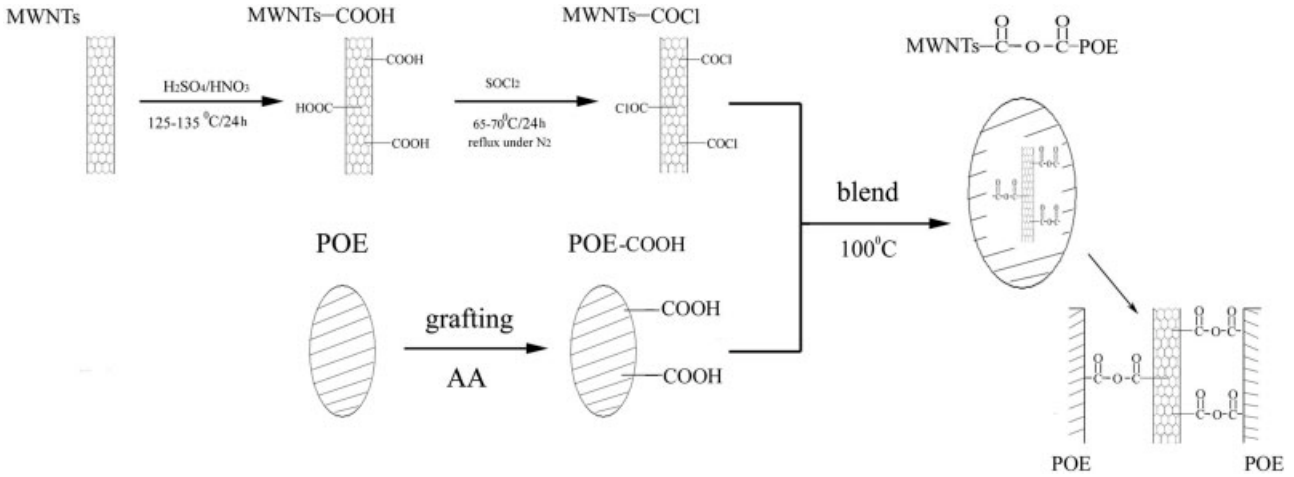

Scheme 1

increasingly important role in the polymer industry. Polyethylene (PE) is one of the most important thermoplastics. However, application of PE is restricted because of its low melting point, its stability, and a tendency to crack when stressed. These disadvantages can be mitigated via grafting reactions, i.e., crosslinking and blending PE with organic fillers. Especially, the metallocene-based polyethylene–octene elastomer (POE), which has been developed by Dow and Exxon using a metallocene catalyst, has received much attention due to its unique uniform distribution of comonomer and narrow molecular weight distribution.[26,27]

Based on the above demonstration and prompted by the observations of 'Kaempfer et al.[28] and Wang et al.[29] on the synthesis and characterization of maleated polypropylene/silicate and maleated polypropylene/clay nanocomposites, it is expected that the incorporation of reinforcing agents such as nanotubes will allow an improvement of some of the properties of these systems. Note that one of the major challenges for producing high performance CNT-reinforced polymer nanocomposites is to optimize the processing operations to have lower cost. Among the commonly used processing techniques, including solution mixing, *in situ* polymerization, and melt compounding,[30–32] the melt compounding method has been accepted as the simplest and most effective one from an industrial perspective. It is because this process makes it possible to fabricate high performance nanocomposites at low cost and also facilitates commercial scale-up.

In this article, we report a new method for covalently linking MWNTs with acrylic acid-grafted metallocene polyethylene–octene elastomer (POE-*g*-AA). MWNTs were first chemically oxidized with strong oxidizing agents such as a mixture of HNO_3 and H_2SO_4, and the generated carboxyls were next converted into acyl chlorides by a treatment with thionyl chlorides. Afterwards, the acyl chloride-functionalized MWNTs reacted with the POE-*g*-AA. This material was then thoroughly characterized with Fourier transform infrared (FTIR), scanning electron microscopy (SEM)/energy-dispersive X-ray spectrometer (EDS), solid state NMR, and thermal analysis techniques.

EXPERIMENTAL

Materials

Pure MWNTs (> 95%, diameter = 40–60 nm), produced via chemical vapor deposition (CVD), were purchased from Seasunnano (China). Sulfuric acid (96%), nitric acid (65%), and thionyl chloride were purchased from Aldrich Chemical. POE (Engage 8003, from Dow Chemical, Wilmington, DE), with 18% octane, was used as received. Acrylic acid (AA, from Aldrich Chemical, Milwaukee, WI) was purified before use via recrystallization from chloroform. The initiator dicumyl peroxide (DCP), also from Aldrich Chemical, was recrystallized twice by dissolving it in absolute methanol. Other reagents were purified using the conventional methods. The POE-*g*-AA copolymer was constructed in our laboratory with a grafting percentage of about 5.65 wt %.

Sample preparation

POE-*g*-AA/MWNTs hybrids

The purity of the purchased MWNTs was 95%. To eliminate the impurities in the MWNTs (such as metallic catalysts), they were treated with 96% H_2SO_4 and 65% HNO_3 at 125–135°C for 24 h, producing MWNTs–COOH, which was then stirred in $SOCl_2$ at 65–70°C for 24 h under refluxing to convert the carboxylic acid into acyl chlorides (Scheme 1). The conversion was accompanied by the formation of two very stable gaseous species, SO_2 and HCl, and suf-

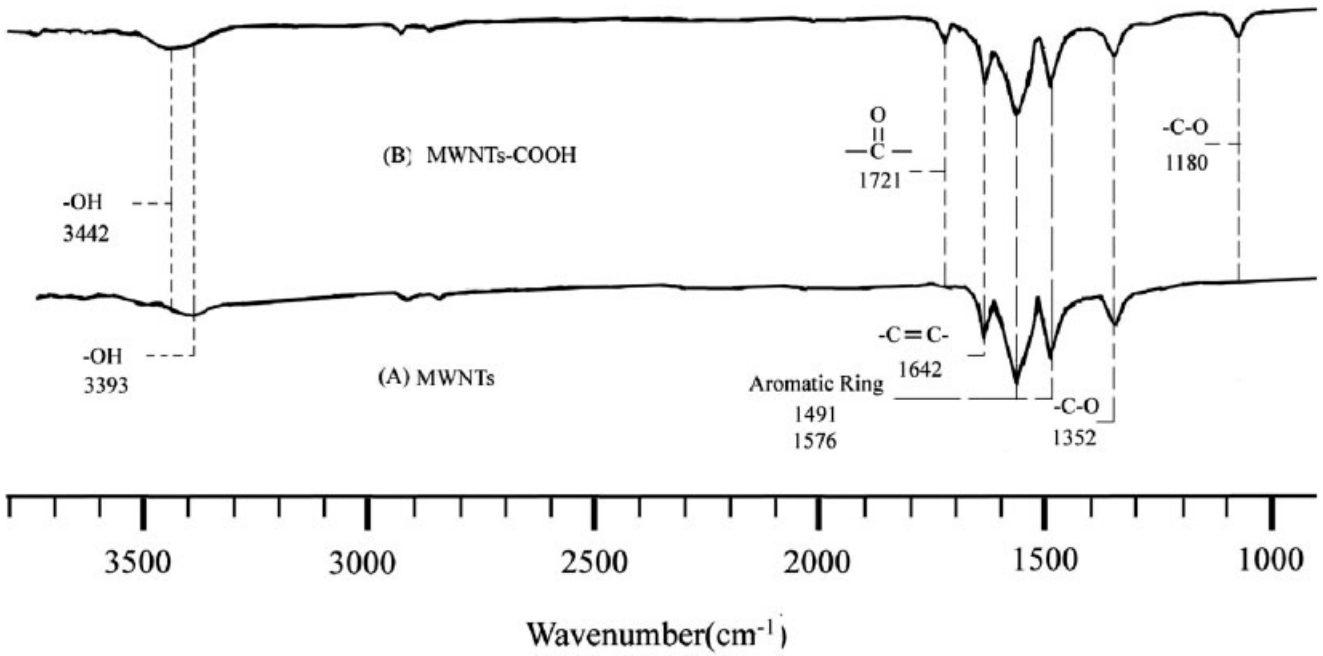

Figure 1 FTIR spectra of (A) pristine MWNTs and (B) MWNTs–COOH.

fered little reverse reaction, because gaseous SO_2 was continuously removed. After the reaction completed, unreacted $SOCl_2$ was evaporated with a rotary evaporator, and the collected MWNTs–COCl samples were dried in a vacuum overnight. With its high reactivity (i.e., low stability), —COCl is hydrolyzed readily into carboxylate ions in air and samples were therefore kept away from air. Prior to preparation of POE-*g*-AA/MWNTs hybrids, the MWNTs–COCl was dried in a vacuum oven at 50°C for 2 days. A Brabender ''Plastograph'' 200 Nm W50EHT mixer with a blade-type rotor (Duisburg, Germany) was used to blend MWNTs–COCl and POE-*g*-AA (mass ratios set at 2.5/97.5, 5/95, 7.5/92.5, and 10/90), with a rotor speed of 50 rpm and a temperature of 100°C, for 15 min. After blending, the composites were pressed into 1-mm-thick films using a hydrolytic press at 100°C and then put into a desiccator for cooling, after which they were made into standard specimens for further characterization.

Characterizations of hybrids

FTIR/NMR/XRD/DSC analysis

The grafting of acrylic acid onto POE was investigated via Fourier transform infrared spectrometry (BIO-RAD FTS-7PC type, Madison, WI), for which the sample was first ground into powder and then coated onto a KBr plate. FTIR analysis also allowed verification of ester bond formation in hybrids and hence verification of the incorporation of a MWNTs–COCl phase. NMR ^{13}C analysis was performed after degassing, at 50 MHz, 90° pulse, and 4-s cycle time, using a Bruker AMX 400 ^{13}C-NMR spectrometer (Germany). Spectra from ^{13}C NMR were observed under cross-polarization, magic angle spinning, and power decoupling conditions. Changes in the crystal structure were analyzed using XRD, in which the X-ray diffraction intensity curves were recorded with a Rigaku D/max 3V X-ray diffractometer (Tokyo, Japan), using Cu Kα radiation, and with a scanning rate 2°/min. Additionally, thermogravimetric analysis (TA Instrument 2010 TGA, New Castle, DE) was used to assess whether organic–inorganic phase interactions influenced thermal degradation of hybrids. Samples were placed in alumina crucibles and tested with a thermal ramp over the temperature range 30–600°C at a heating rate of 20°C/min and then the initial decomposition temperature (IDT) of hybrids was obtained.

Mechanical test

An Instron mechanical tester (Model Lloyd, LR5K type) was used to measure the tensile strength at break, following the ASTM D638 method. Film samples, prepared via a hydraulic press at 100°C and preconditioned at (50 ± 5)% relative humidity for 24 h, were tested at a 20 mm/min crosshead speed. All tests were repeated five times and a mean value obtained.

Composite morphology

Subsequent to mechanical analysis, films were treated with hot water at 80°C for 24 h, coated with gold, and

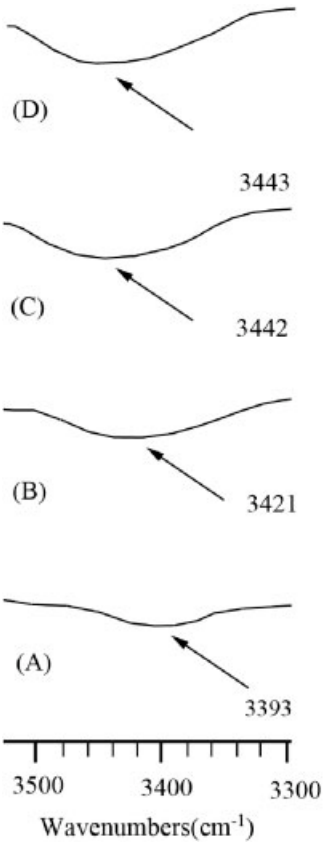

Figure 2 FTIR spectra of MWNTs treated by acid at 125–135°C with various treatment time: (A) 0 h; (B) 12 h; (C) 24 h; (D) 36 h.

their morphology studied using a Hitachi Microscopy Model S-4100 (Japan) scanning electron microscope.

RESULTS AND DISCUSSION

Infrared/NMR spectroscopy

Figure 1 shows the FTIR spectra of MWNTs and MWNTs–COOH. All the peaks, characteristic of MWNTs, at 1600–1450 cm^{-1} (aromatic ring), 1352 cm^{-1} (—C—O), 3393 cm^{-1} (—OH), and 1642 cm^{-1} (—C=C—), appear in both spectra. Closer inspection revealed two unique peaks in the spectrum of MWNTs–COOH, one appearing around 1721 cm^{-1}, arising from the stretching vibration of the C=O group,[12,33] and one at 1180 cm^{-1}, arising from the stretching vibration of the C=O group, both therefore due to the existence of —COOH caused by chemical oxidation when treated with acid. To better understand the carboxylic acid-functionalized MWNTs, the expanded FTIR spectra between 3300 and 3500 cm^{-1} was inspected. Figure 2 shows the hydroxyl-stretching band of MWNTs as a strong broad band at 3393 cm^{-1} [Fig. 2(A)] and, after treatment with acid (96% H_2SO_4/65% HNO_3) at 125–135°C for 12, 24, and 36 h, as a broadening band shifting to 3421, 3442, and 3443 cm^{-1}, respectively. Furthermore, the amount of hetero-associated —COOH leveled off if MWNTs were treated for more than 24 h with acid, making 24 h at 125–135°C a feasible treatment for creating —COOH groups in MWNTs. In essence, these results corroborated the successful carboxylation of MWNTs. Subsequently, upon reacting with thionyl chloride ($SOCl_2$), the —COOH was transformed into acyl chloride functional groups, and the distinctive stretching vibration of —COCl should have been observed. However, the high hydrolytic reactivity of —COCl in air tended to convert this back into carboxylate ions, and this made FTIR detection (operated in air) of the stretching vibration of —COCl extremely difficult. Nevertheless, the condensation reaction between MWNTs–COCl and POE–COOH, exhibited in the FTIR spectrum of MWNTs–COOOC–POE, is indicated by either diminished peaks or no peaks at around 1721 cm^{-1} [Fig. 3(B)]. In contrast, strong absorption for aromatics[34,35] in the region of 1600–1470 cm^{-1} and 1643 cm^{-1} (—C=C—) occurred as a result of the condensation reaction of POE-*g*-AA.

All the FTIR peaks, characteristic of POE-*g*-AA, at 2840–2928 and 1465 cm^{-1}, appear in both POE-*g*-AA

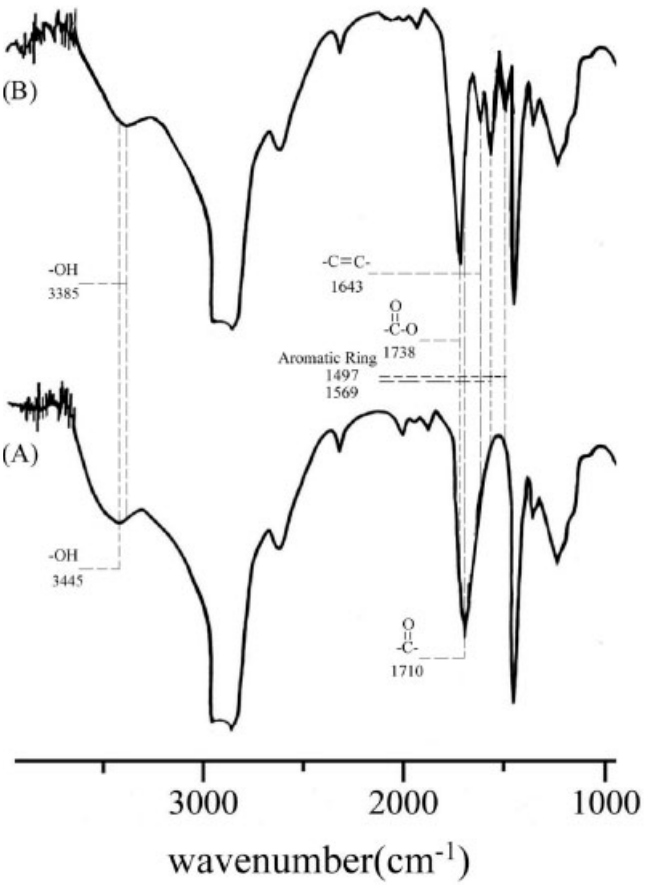

Figure 3 FTIR spectra of (A) POE-*g*-AA and (B) POE-*g*-AA/MWNTs (5 wt %).

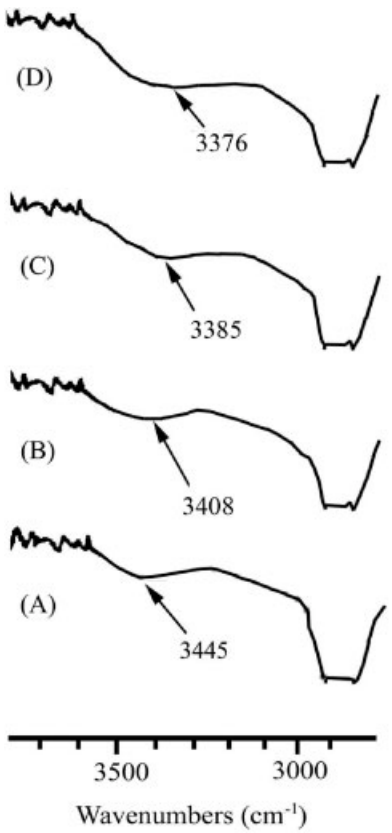

Figure 4 FTIR spectra of (A) POE-*g*-AA/MWNTs (0 wt %), (B) POE-*g*-AA/MWNTs (2.5 wt %), (C) POE-*g*-AA/MWNTs (5 wt %), and (D) POE-*g*-AA/MWNTs (10 wt %).

and POE-*g*-AA/MWNTs (5 wt %) polymers (Fig. 3). Unique peaks were identified at about 3200–3600 and 1000–1800 cm^{-1} in the spectrum of POE-*g*-AA/MWNTs [Fig. 3(B)] and at 1710 cm^{-1} in the spectrum of POE-*g*-AA [Fig. 3(A)]. The peak at 1710 cm^{-1} in POE-*g*-AA was replaced by a peak at 1738 cm^{-1} in POE-*g*-AA/MWNTs, and this is due to the formation of ester groups through the condensation reaction between carboxylic acid groups of POE-*g*-AA and acyl chloride groups of the MWNTs–COCl.[36] Additionally, the hydroxyl-stretching band appears as a strong broad band at 3445 cm^{-1} in the POE-*g*-AA copolymer, while for POE-*g*-AA/MWNTs hybrids, the vibration band broadened and shifted to 3385 cm^{-1}. The reason for this shift in wave number is the presence of HCl formed from esterification of —COOH and —COCl.

Figure 4 further shows the effect of MWNT content on the hydroxyl-stretching band of POE-*g*-AA/MWNTs. For the POE-*g*-AA copolymer, the hydroxyl-stretching band appears as a strong broad band at 3445 cm^{-1} [Fig. 4(A)], whereas for POE-*g*-AA/MWNTs–COCl hybrids, the vibration bands broadened with MWNTs–COCl content at 2.5, 5, and 10 wt % and shifted to 3408, 3385, and 3376 cm^{-1}, respectively. The above observations demonstrate the existence of strong hetero-associated hydrogen bonds between carboxylic acid groups of the POE-*g*-AA matrix and carbonyl groups of MWNTs–COCl. Because of the formation of an ester group, the —COOH group decreased with increase in MWNTs–COCl content, conferring a shift of the wave number to a lower value (lower stretching energy). Another reason for the shift in wave number is the presence of HCl formed from esterification of —COOH and —COCl, which also increased with MWNTs–COCl content.

A further understanding of the condensation between POE-*g*-AA and MWNTs was achieved using ^{13}C NMR to study structural changes of hybrids. Figure 5 shows the solid-state ^{13}C NMR spectra of POE-*g*-AA [Fig. 5(A)], POE-*g*-AA/MWNTs [Fig. 5(B)], MWNTs–COOH [Fig. 5(C)], and MWNTs [Fig. 5(D)]. The spectrum of POE-*g*-AA corresponds with those reported elsewhere,[37] as does that of MWNTs.[38] Peaks at $\delta = 120$–125 ppm present in the spectrum of POE-*g*-AA/MWNTs but not in POE-*g*-AA were due to the aromatic carbon of MWNTs, while peaks at C_α, C_β, and $\delta = 175.042$ ppm were caused by grafting of AA onto POE, as was indicated by Wu et al.[37] The peak at $\delta = 175.042$ ppm (C=O) in the spectrum of POE-*g*-AA shifted to $\delta = 177.056$ ppm in POE-*g*-AA/MWNTs, due to the reaction between —COOH and —COCl in the latter. This provides further evidence of the condensation between POE-*g*-AA and MWNTs–COCl, and leads to the conclusion that the original MWNTs–COCl was fully acylated, and that in this reaction the acyl chloride groups were converted to ester. Formation of ester functional groups has a profound effect on thermal and mechanical properties, something that will be discussed in the following sections.

^{13}C NMR spectroscopy also enabled a characterization of the insoluble samples directly from a uniform powder without a deuterated solvent. The small signal seen at ~ 166.569 ppm in the spectrum of MWNTs [Fig. 5(D)] is caused by the inherent carboxylate (—COOR) group of MWNTs, a product of the acid used in its construction.[12] In Figure 5(C) (MWNTs–COOH), this peak is seen shifted to 167.876 ppm because of the removal of Ni (as shown in Table I) and, measured at the same signal-to-noise ratio, is also more intense. The increased intensity thus confirmed the additional carboxylation of MWNTs via chemical

TABLE I
SEM/EDS Data

Sample	C (wt %)	O (wt %)	Cl (wt %)	Ni (wt %)
Pure MWNTs	96.69	1.83	–	1.48
MWNTs–COOH	90.02	9.98	–	–
MWNTs–COCl	88.56	8.96	2.48	–
MWNTs–COOOC–POE	93.61	6.18	0.21	–

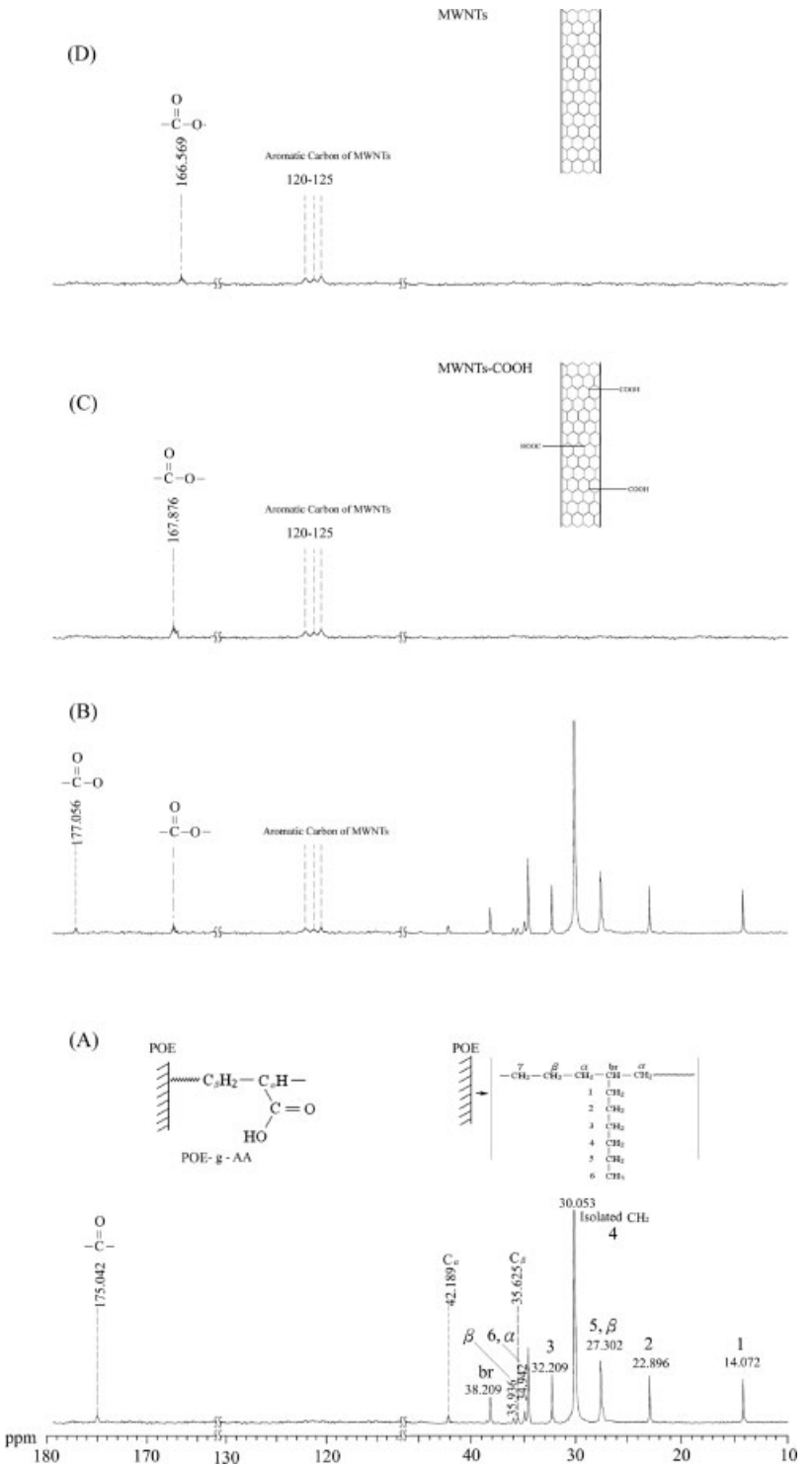

Figure 5 ^{13}C solid-state NMR spectra of (A) POE-*g*-AA, (B) POE-*g*-AA/MWNTs (5 wt %), (C) MWNTs–COOH, and (D) MWNTs.

oxidation. Signals associated with POE-*g*-AA can be seen in both Figure 5(A,B). A comparison of the downfield of the spectra for MWNTs–COOH [Fig. 5(C)] and POE-*g*-AA/MWNTs [Fig. 5(B)], meanwhile, reveals that the signal at ~ 167.87 ppm decreased significantly in the latter because of the attack of POE-*g*-AA on the carbonyl group. These signal changes in the spectra served as direct evidence for the functionalization of POE-*g*-AA.

X-ray diffraction

X-ray diffraction was used to examine the crystalline structures of pure POE-*g*-AA, POE-*g*-AA/MWNTs

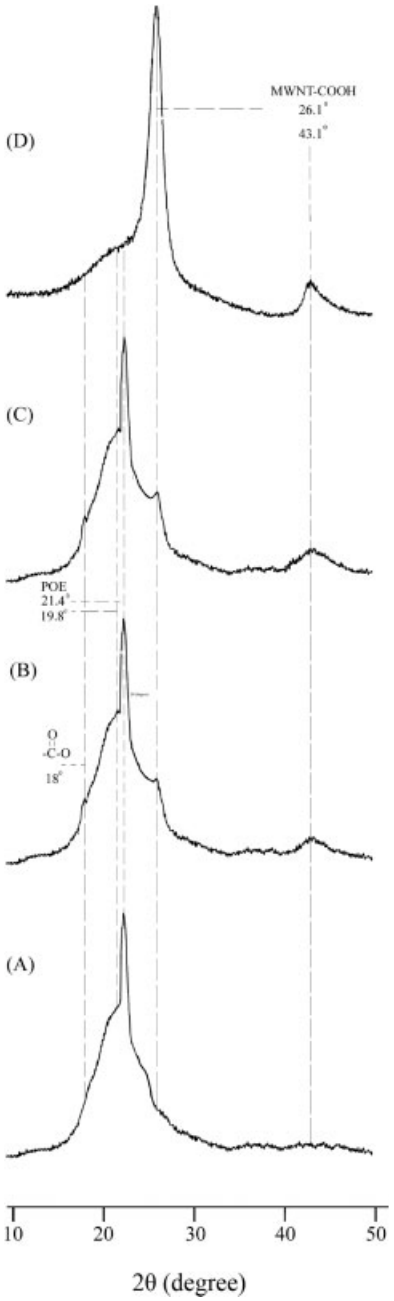

Figure 6 X-ray diffraction spectra of (A) pure POE, (B) POE-*g*-AA/MWNTs (5 wt %), (C) POE-*g*-AA/MWNTs (10 wt %), and (D) MWNTs–COOH.

(2.5 wt %), POE-*g*-AA/MWNTs (5 wt %), and MWNTs [Fig. 6(A)–6(D), respectively]. While for unmodified POE there is a peak at about $2\theta = 19.8^\circ$, considered indicative of the side branches of octene, and another at about $2\theta = 21.4^\circ$, representing the orthombic cells of polyethylene,[37] all forms of the POE-*g*-AA copolymer produced only the latter peak (Fig. 6), and this may be due to changes in coordination features of POE molecules when acrylic acid is grafted onto POE.

Four peaks not present in POE-*g*-AA are apparent in the POE-*g*-AA/MWNTs hybrids, at $2\theta = 18.0^\circ$, 19.8°, 26.1°, and 43.1°. The peak at $2\theta = 18.0^\circ$ may be due to the formation of an ester carbonyl functional group, as described in the discussion of FTIR analysis, and is similar to that reported by Wu and Liao.[36] Condensation between POE-*g*-AA and MWNTs–COCl also caused the reappearance of a peak at $2\theta = 19.8^\circ$, which is due to recovery of POE characteristics with the consumption of AA in the POE-*g*-AA. Because the peaks at $2\theta = 26.1^\circ$ and 43.1° in the spectrum of MWNTs–COOH [Fig. 6(D)], similar to those reported by Fan et al.,[39] are also apparent in Spectrums B and C, one can relate these peaks to the existence of a MWNTs–COOH phase,[40] which was attributed to the generation of a MWNTs–COOC–POE functional group in the POE-*g*-AA condensation reaction. It was also noted that these peaks became larger as MWNTs–COOH content increased.

TGA measurements

It is known that the defunctionalization of carbon nanotubes can be realized by thermal decomposition. In the present study, we used thermogravimetry analysis (TGA, 20°C/min) to determine the effects of a relative amount of MWNTs–COCl on decomposition of POE-*g*-AA/MWNTs. Figure 7 shows the TGA traces of POE-*g*-AA, POE-*g*-AA/MWNTs (5 wt %), POE-*g*-AA/MWNTs (10 wt %), and MWNTs, under nitrogen. The initial degradation temperature (IDT) of pure POE-*g*-AA was 403°C, and the value of this parameter increased with MWNT content, whereas the IDT of POE-*g*-AA/MWNTs (5 wt %) and POE-*g*-AA/MWNTs (10 wt %) blends was delayed until 450 and 472°C, respectively, whereupon the weight of these composites decreased rapidly (Fig. 7), because of the decomposition of POE-*g*-AA. The difference in temperature required for thermal decomposition was probably due to MWNTs having a more prohibitive

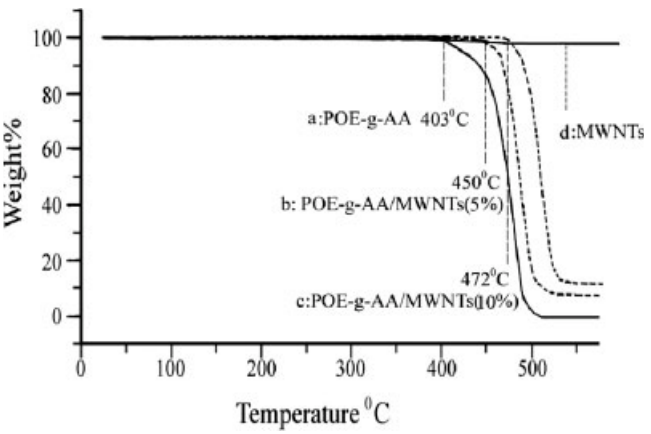

Figure 7 TGA curves of (A) pure POE, (B) POE-*g*-AA/MWNTs (5 wt %), (C) POE-*g*-AA/MWNTs (10 wt %), and (D) MWNTs–COOH.

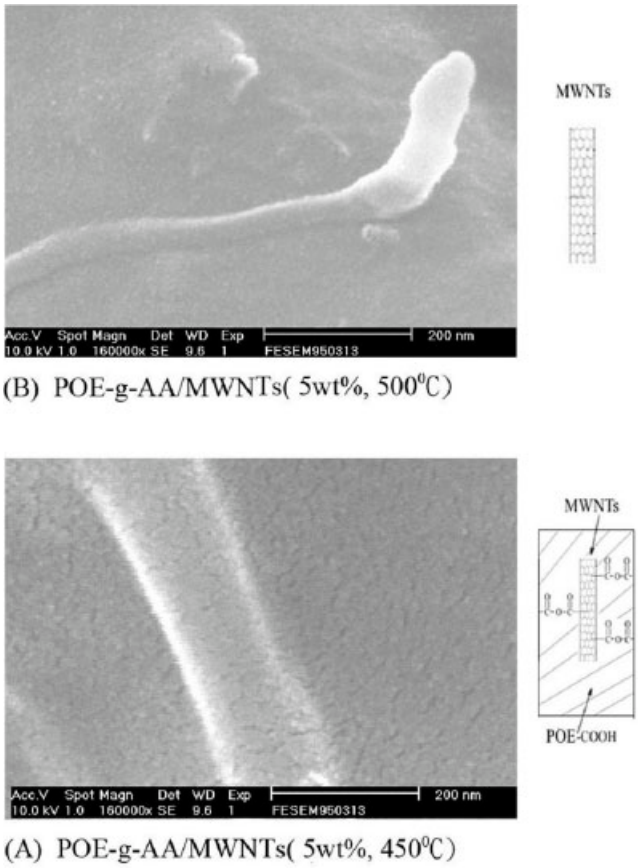

Figure 8 SEM micrographs of POE-*g*-AA/MWNTs (5 wt %) subjected to TGA at (A) 450°C and (B) 500°C.

effect on movement of the polymer segments at higher weight percent. Another potential cause is the character of MWNTs–COCl, which leads to condensation reaction with the POE-*g*-AA. Kashiwagi et al.[41] studied the properties of clay nanocomposite and its blends with polypropylene, and reported similar phenomena.

Neat MWNTs did not degrade even at temperatures above 500°C (Fig. 7). This observation supports the conclusion that weight loss of the composites was due to decomposition of POE-*g*-AA. Furthermore, the residual yields of the POE-*g*-AA/MWNTs nanocomposites increased with increasing MWNT content (0, 8, and 15 wt % residual yield for 0, 5, and 10 wt % MWNTs, respectively), indicating that thermal decomposition of the polymer matrix was retarded in the POE-*g*-AA/MWNTs nanocomposites. This result may be attributed to a physical barrier effect, resulting from the fact that MWNTs would prevent the transport of decomposition products in the polymer nanocomposites. Thermal stability of polypropylene/MWNTs nanocomposites was also improved by a physical barrier effect, enhanced by MWNT layer.[42] The TGA results therefore demonstrate that the incorporation of a small quantity of MWNTs can significantly improve the thermal stability of POE-*g*-AA/MWNTs nanocomposites.

Additionally, SEM images revealed that MWNTs were covered with amorphous POE-*g*-AA, supporting the conclusion that POE-*g*-AA was covalently bonded to the walls of MWNTs. Figure 8(A) shows an SEM image of POE-*g*-AA/MWNTs after it was subjected to TGA up to 450°C. The amorphous POE-*g*-AA covering the MWNTs (5 wt %) faded after being heated to 450°C, although some residual was observed, conferring a larger diameter on the POE-*g*-AA/MWNTs when compared with that heated to 500°C [Fig. 5(B)].

Hybrid morphology

It is necessary to study the morphology of the MWNTs and polymer blends, since the mechanical properties depend on it. In general, good dispersion of MWNTs in the matrix and strong interfacial adhesion between the two phases are required to obtain a composite material with satisfactory mechanical properties. Scanning electron microscopy was used to study the tensile fracture surfaces of composite samples of POE-*g*-AA/MWNTs (5 wt %) blends, in which the major component (POE-*g*-AA) forms the matrix and the minor component (MWNTs) the dispersed phase.

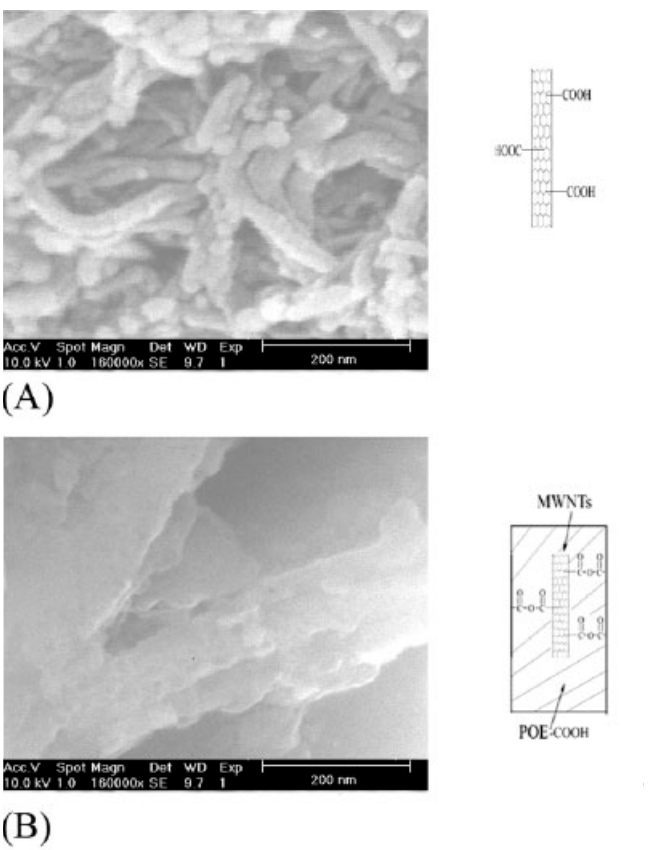

Figure 9 SEM micrographs of (A) MWNTs–COOH and (B) tensile fracture surfaces of POE-*g*-AA/MWNTs (5 wt %).

In Figure 9(B) (POE-*g*-AA/MWNTs), MWNTs can be seen embedded in the POE-*g*-AA matrix, and smooth interfaces between MWNTs and POE-*g*-AA are observed, so that the MWNTs are considered to have good wettability for POE-*g*-AA, albeit with some absence of physical contact, considered due to insufficient condensation reaction between MWNTs–COCl and POE-*g*-AA. There is therefore adequate dispersion and homogeneity of MWNTs in the POE-*g*-AA matrix. In contrast, the entangled clusters seen in the SEM photo of MWNTs–COOH [Fig. 9(A)] are the result of insufficient dispersion and poor interfacial adhesion between filler and matrix. Better wetting is also obtained with the POE-*g*-AA/MWNTs, as evidenced by the matrix material having been pulled out together with the MWNTs–COCl. Adhesion between the two phases is also responsible for the observed diameter differences: the diameters of POE-*g*-AA/MWNTs (5 wt %) are larger, at 80–150 nm.

Tensile strength of hybrids

Tensile strength of the POE-*g*-AA/MWNTs nanocomposites at different MWNT weight percent content is shown in Figure 10. Tensile strength increased noticeably when MWNT content was increased from 0 to 2.5 wt % and from 2.5 to 5 wt %, after which it approached a stable value with further 2.5 wt % increase. This positive effect on tensile strength may be due to the stiffness of the MWNTs layers contributing to the presence of immobilized or partially immobilized polymer phases[43] and to the nanoscale dispersion of MWNTs layers in the polymer matrix. It is also possible that MWNT layer orientation as well as molecular orientation contributes to the observed reinforcement effect. However, MWNTs often tend to bundle together because of intrinsic van der Waals attraction between the individual tubes in combination with high aspect ratio and surface area of the nanotubes, leading to some agglomeration on the polymer matrix.[5,44] Indeed, the leveling off in tensile strength seen at MWNT content above 5 wt % could be attributed to the inevitable aggregation of the nanotubes at higher contents, and this might indicate an upper limit to the amount of MWNTs that can be added directly into POE-*g*-AA if a significant increase in viscosity and probably also a saturation of nanotube addition[27] is to be avoided. Alternatively, ways might be found to improve the dispersion of MWNTs in the POE-*g*-AA matrix and the interfacial adhesion between the MWNTs and the POE-*g*-AA matrix via functionalization of MWNTs, and we are currently exploring this topic.

Observed increases in tensile strength reflect strong interfacial bonding due to the free terminal acyl chloride groups covalently attached to the side chains of MWNTs, conferring chemical bonding of these groups to the POE-*g*-AA matrix. These results demonstrate that stress transfer, and hence strength, of nanotube-polymer composites can be effectively increased by addition of chemical bonding.[45,46] This is most likely due to some void defects, suggesting more room for improvement. It should be mentioned that in this work the functionalization route used, adding carboxyl-terminated free radicals to the nanotubes, was nondestructive to the sidewall: during the first step of functionalization, we effectively controlled the time of acid treatment to maintain wall integrity. In comparison, sidewall carboxylation by using a relatively long oxidative treatment time might destroy the wall integrity and would likely affect the tensile strength of both the nanotubes and polymer composites made with them.

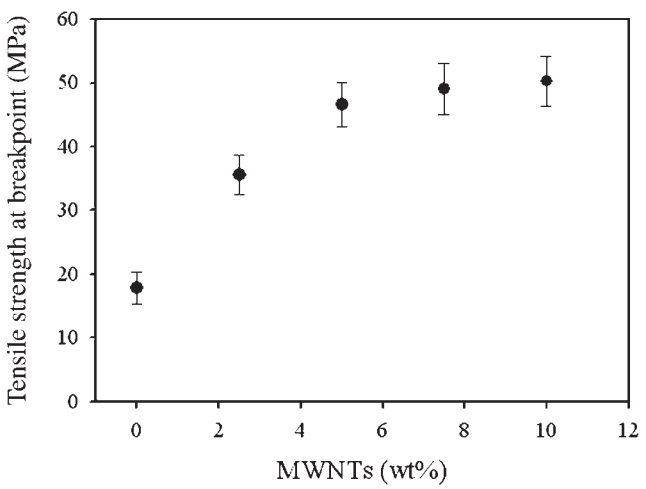

Figure 10 Tensile strength at breakpoint versus MWNTs content for POE-*g*-AA/MWNTs hybrids.

CONCLUSIONS

Via processes involving carbon nanotubes sidewall and end-tip functionalization steps, POE-*g*-AA composite preparation, and a condensation reaction, a fully integrated POE-*g*-AA/MWNTs composite material was prepared for structural applications. Acyl chloride functionalization provided the nanotubes with a very effective side chain. As a result, MWNTs–COCl can be incorporated into POE-*g*-AA for producing an effective system in which MWNTs will play a reinforcement role in the polymer matrix. The results obtained through integration of functionalized nanotubes demonstrate significant improvement in mechanical properties of the POE-*g*-AA system. The polymer-multiple-walled carbon nanotube hybrid materials developed in this article were prepared using a melting process. A number of reactive functional groups are capable of attaching covalently to

polymers, and the technology for developing fully integrated nanotubes and POE-*g*-AA polymer composites by functionalization can therefore be extended to other polymer systems to provide a variety of hybrid materials. FTIR, ^{13}C solid-state NMR, and XRD spectra showed that the acrylic acid had been grafted onto the POE copolymer and that ester bonds had formed in the POE-*g*-AA/MWNTs hybrid. The newly formed ester bonds may be produced through condensation of carboxylic acid groups in the POE-*g*-AA matrix with grafted acyl chloride groups in the acid-treated MWNTs. TGA tests showed that the addition of MWNTs to POE-*g*-AA raised the IDT and the tensile strength. Values of tensile strength leveling off at about 5 wt % MWNTs, and excess MWNTs above this weight percent caused aggregation of the MWNT phase and so reduced compatibility between the grafted acyl chloride groups in the acid-treated MWNTs and POE-*g*-AA. Finally, the POE-*g*-AA/MWNTs hybrids showed improved thermal and mechanical properties, because the interfacial forces of POE-*g*-AA are the stronger covalent bonds. Moreover, comparing the works of Kaempfer et al.[28] and Chen et al.,[47] where clay and carbon black were used as additives respectively, the present study showed a lower additive content to attain the optimal performance (10 wt % compared with 5 wt %).

References

1. Treacy, M. M. J.; Ebbesen, T. W.; Gibson, J. M. Nature 1996, 381, 678.
2. Coleman, J. N.; Khan, U.; Gun'ko, Y. K. Adv Mater 2006, 18, 689.
3. Fan, S.; Chapline, M. G.; Franklin, N. R.; Tombler, T. W. Science 1999, 283, 512.
4. Iijima, S. Nature 1991, 354, 56.
5. Chen, J.; Ramasubramaniam, R.; Xue, C.; Liu, H. Adv Funct Mater 2006, 16, 114.
6. Zeng, H.; Gao, C.; Wang, Y.; Watts, P. C. P.; Kong, H.; Cui, X.; Yan, D. Polymer 2006, 47, 113.
7. Ajayan, P. M.; Stephan, Q.; Colliex, C.; Trauth, D. Science 1994, 265, 1212.
8. Shaffer, M. S. P.; Windle, A. H.; Iijima, S. Adv Mater 1999, 11, 937.
9. Fisher, F. T.; Bradshaw, R. D.; Brinson, L. C. Appl Phys Lett 2002, 80, 4647.
10. Leelapornpisit, W.; Ton-That, M. T.; Ferrin-Sarazin, F.; Cole, K. C.; Denault, J.; Simard, B. J Polym Sci Part B: Polym Phys 2005, 43, 2445.
11. Zhang, W. D.; Shen, L.; Phang, I. Y.; Liu, T. Macromolecules 2004, 37, 256.
12. Bellayer, S.; Gilman, J. W.; Eidelman, N.; Bourbigot, S.; Flambard, X.; Fox, D. M.; Long, H. C. D.; Trulove, P. C. Adv Funct Mater 2005, 15, 910.
13. Wu, H. L.; Yang, Y. T.; Ma, C. C. M.; Kuan, H. C. J Polym Sci Part A: Polym Chem 2005, 43, 6084.
14. Cui, S.; Canet, R.; Derre, A.; Couzi, M.; Delhaes, P. Carbon 2003, 41, 797.
15. Huang, H. M.; Lin, I. C.; Chang, C. Y.; Tsai, H. C.; Hsu, C. H.; Tsiang, R. C. J Polym Sci Part A: Polym Chem 2004, 42, 5802.
16. Chen, J.; Hamon, M. A.; Hu, H.; Chen, Y.; Rao, A. M.; Eklund, P. C.; Haddon, R. C. Science 1998, 282, 95.
17. Kim, H. S.; Jin, H. J.; Myung, S. J.; Kang, M.; Chin, I. J. Macromol Rapid Commun 2006, 27, 146.
18. Lin, J.; Rinzler, A. G.; Dai, H.; Hafner, J. H.; Bradley, R. K.; Boul, P. J.; Lu, A.; Iverson, T.; Shelimov, K.; Huffman, C. B.; Rodriguez-Macias, F.; Shon, Y. S.; Lee, T. R.; Colbert, D. T.; Smalley, R. E. Science 1998, 280, 1253.
19. Yoon, K. R.; Kim, W. J.; Choi, I. S. Macromol Rapid Commun 2004, 205, 1218.
20. Thess, A.; Lee, R.; Nikoaev, P.; Dai, H.; Robert, J.; Xu, C.; Lee, Y. H.; Kim, S. G.; Rinzler, A. G.; Colbert, D. T.; Scuseria, G. E.; Tomanek, D.; Fisher, J. E.; Smalley, R. E. Science 1996, 273, 483.
21. Chen, S.; Wu, G.; Liu, Y.; Long, D. Macromolecules 2006, 39, 330.
22. Jung, Y. C.; Sahoo, N. G.; Cho, J. W. Macromol Rapid Commun 2006, 27, 126.
23. Hill, D. E.; Lin, Y.; Rao, A. M.; Allard, L. F.; Sun Y. P. Macromolecules 2002, 35, 9466.
24. Jammak, J.; Cheng, S.; Zhang, A.; Hsieh, E. Polymer 1992, 33, 728.
25. Valentini, L.; Biagiotti, J.; Kenny, J. M.; Manchado, M. A. L. J Appl Polym Sci 2003, 89, 2657.
26. Bensason, S.; Nazarenko, S.; Chum, S.; Hiltner, A.; Baer, E. Polymer 1997, 38, 3913.
27. Wu, C. S. J Polym Sci Part A: Polym Chem 2005, 43, 1690.
28. Kaempfer, D.; Thomann, R.; Mulhaupt, R. Polymer 2002, 43, 2909.
29. Wang, K. H.; Choi, M. H.; Koo, C. M.; Choi, Y. S.; Chung, I. J. Polymer 2001, 42, 9819.
30. Potschke, P.; Fornes, T. D.; Paul, D. R. Polymer 2002, 43, 3247.
31. Park, S. J.; Cho, M. S.; Lim, S. T.; Choi, H. J.; Jhon, M. S. Macromol Rapid Commun 2003, 24, 1070.
32. Sarno, M.; Gorrasi, G.; Sannino, D.; Sorrentino, A.; Ciambelli, P.; Vittoria V. Macromol Rapid Commun 2004, 25, 1963.
33. Kuznetsova, A.; Mawhinney, D. B.; Naumenko, V.; Yates, J. T., Jr., Li, Q.; Smalley, R. E. J Phys Chem B 2000, 321, 292.
34. Zhu, J.; Peng, H.; Fernando, R.-M.; Margrave, J. L.; Khabashesku, V. N.; Imam, A. M.; Lozano, K.; Barrera, E. V. Adv Funct Mater 2004, 14, 643.
35. Liu, I.-C.; Huang, H. M.; Chang, C.-Y.; Tsai, H.-C.; Hsu, C.-H.; Tsiang, R. C.-C. Macromolecules 2004, 37, 283.
36. Wu, C. S.; Liao, H. T. J Polym Sci Part B: Polym Phys 2003, 41, 351.
37. Wu, C. S.; Lai, S. M.; Liao, H. T. M. J Appl Polym Sci 2002, 85, 2905.
38. Zhu, J.; Kim, J.; Peng, H.; Margrave, J. L.; Khabashesku, V. N.; Barrera, E. V. Nano Lett 2003, 3, 1107.
39. Fan, J.; Wax, M.; Zhu, D.; Chang, B.; Pan, Z.; Xiz, S. J Appl Polym Sci 1999, 74, 2605.
40. Wildgoose, G. G.; Wilkins, S. J.; Williams, G. R.; France, R. R.; Carnahan, D. L.; Jiang, L.; Jones, T. G. J.; Compton, R. G. ChemPhysChem 2005, 6, 352.
41. Kashiwagi, T.; Grulke, E.; Hilding, J.; Harris, R.; Awad, W.; Douglas J. Macromol Rapid Commun 2002, 23, 761.
42. Bom, D.; Andrews, R.; Jacques, D.; Anthony, J.; Chen, B.; Meier, M. S.; Selegue, J. P. Nano Lett 2002, 2, 615.
43. Zhang, X.; Liu, T.; Sreekumar, T. V.; Kumar, S.; Moore, V. C.; Hauge, R. H.; Smalley, R. E. Nano Lett 2003, 3, 1285.
44. Coleman, J. N.; Cadek, M.; Blake, R.; Nicolosi, V.; Ryan, K. P.; Belton, C.; Fonseca, A.; Nagy, J. b.; Cun'ko, Y. K.; Blau, W. J. Adv Funct Mater 2004, 14, 791.
45. Geng, H.; Rosen, R.; Zheng, B.; Shimoda, H.; Fleming. L.; Liu, J.; Zhou, O. Adv Mater 2002, 14, 1387.
46. Yao, Z.; Braidy, N.; Botton, G. A.; Adronov, A. J Am Chem Soc 2003, 125, 16015.
47. Chen, C. H.; Li, H. C.; Teng, C. C.; Yang, C. H. J Appl Polym Sci 2006, 99, 2167.